FPMC2019-1693

EXPERIMENTAL TESTING OF A VARIABLE DISPLACEMENT PUMP/MOTOR THAT USES A HYDRO-MECHANICALLY TIMED DIGITAL VALVING MECHANISM TO ACHIEVE PARTIAL-STROKE PISTON PRESSURIZATION (PSPP)

Alissa Montzka, Nathan Epstein, Michael Rannow * Thomas R. Chase, and Perry Y. Li

Department of Mechanical Engineering University of Minnesota Minneapolis, MN 55455

ABSTRACT

This work describes an efficient means to adjust the power level of an axial piston hydraulic pump/motor. Conventionally, the displacement of a piston pump is varied by changing the stroke length of each piston. Since the losses do not decrease proportionally to the displacement, the efficiency is low at low displacements. Here, with partial-stroke piston pressurization (PSPP), displacement is varied by changing the portion of the piston stroke over which the piston is subjected to high pressure. Since leakage and friction losses drop as the displacement is decreased, higher efficiency is achieved at low displacements with PSPP. While other systems have implemented PSPP with electric or cam-actuated valves, the pump described in this paper is unique in implementing PSPP by way of a simple, robust hydromechanical valve system. Experimental testing of a prototype PSPP pump/motor shows that the full load efficiency is maintained even at low displacements.

INTRODUCTION

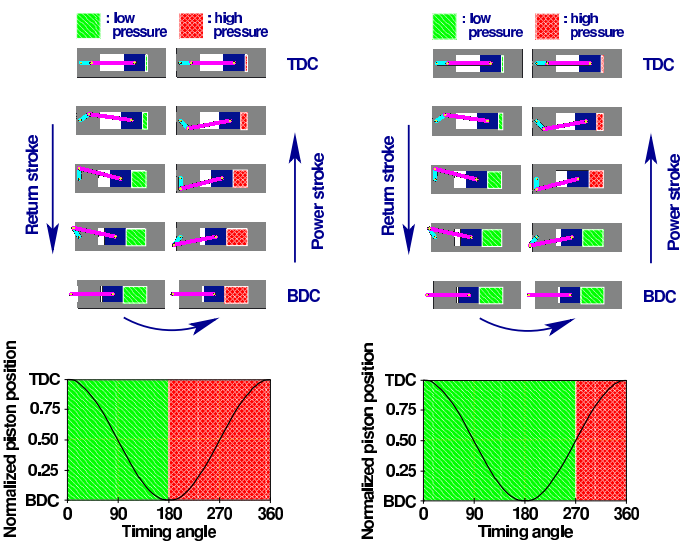
Hydraulic systems are useful in a variety of applications where high power density and ruggedness are desired, but typically they are less efficient than competing technologies. This lower efficiency is due to the use of throttling valves and friction and leakage within pumps and motors. System efficiency

can be increased by utilizing variable displacement pumps and motors. Variable displacement devices are typically designed to reach peak efficiency at full displacement. However, losses do not generally scale down in proportion to displacement, so the efficiency drops substantially at lower displacements. On the other hand, if the displacement is adjusted by judiciously removing pressure from the piston chambers, then the losses can be made to largely scale with displacement so that efficiency can be kept high even at low displacements. This approach is referred to as partial-stroke piston pressurization (PSPP).

Many approaches in the so-called digital displacement machines utilize electronically controlled electromagnetic valves (usually two per piston). In one of the first works on the subject [1] [2], to satisfy a flow demand signal whole pistons are enabled or disabled on a stroke-by-stroke basis. In [3] a dynamic model drives the design of a pump/motor employing actively controlled high speed on/off valves. A three-piston digital displacement pump/motor has been tested using algorithms to vary the displacement in flow-diverting and flow-limited operating strategies [4]. In [5] the pistons are each controlled independently. This can increase cost and complexity, and reduce robustness. The novel pump/motor described here employs a simple, robust hydro-mechanical valve [6] [7] to implement PSPP. In this design, a single 2D rotary on/off valve is used as a pilot valve. The valve has two degrees of freedom. It rotates with the shaft of the pump/motor, and it also translates axially to control the displacement of the unit. The rotary valve sends pilot pressure sig-

_____ th

^{*}Currently at Eaton Corp., 14900 Technology Dr, Eden Prairie, MN 55344 †Send all correspondence to this author.



(a) Normal pumping cycle of any piston pump, including a PSPP pump running at full displacement.

(b) Pumping cycle of a PSPP pump operating at 50% displacement.

FIGURE 1: Basic operating principle of partial-stroke piston pressurization pumps. The piston has a constant stroke length. Displacement is reduced by reducing the portion of the power stroke where the piston cylinder is connected to the high pressure line.

nals to actuate main stage spools (one per piston) that ultimately connect and disconnect the piston chamber to high pressure or tank pressure.

The subsequent sections present the principles of operation and experimental results for a PSPP pump/motor, operated exclusively in pumping mode, in the following order. The concept of using PSPP to vary the displacement of a pump is reviewed. The architecture of the first prototype pump/motor is introduced. The testing apparatus and procedure are described. Experimental results are presented and compared with simulated results.

PARTIAL STROKE PISTON PRESSURIZATION

The concept of partial-stroke piston pressurization is introduced in Fig. 1. For simplicity, this figure assumes that the pump/motor has a slider-crank architecture, although PSPP works equally well for any piston displacement mechanism. Figure 1a illustrates the normal pumping cycle of any piston pump, including a PSPP pump running at full displacement. Low pressure fluid is drawn in to the piston cylinder on the return stroke. High pressure fluid is pushed out of the piston cylinder for nominally the entirety of the power stroke.

Most variable displacement piston pumps reduce the displacement by reducing the stroke length of the piston. High pres-

sure is applied to the piston for the entire power stroke, regardless of the piston displacement. In contrast, the stroke length of the piston of a PSPP pump remains constant regardless of the displacement setting. Displacement is reduced by delaying the application of high pressure to the piston cylinder until the piston has moved partially up the power stroke.

The pumping cycle of a PSPP pump operating at 50% displacement is illustrated in Fig. 1b. A valve connecting the piston cylinder to the low pressure fluid supply remains open for the first half of the power stroke, while a valve connecting the piston cylinder to the high pressure fluid outlet remains closed. Low pressure fluid in the piston cylinder is shuttled back out to the low pressure fluid supply, but still at low pressure, as the piston rises. When the piston reaches half its displacement between bottom dead center (BDC) and top dead center (TDC), the low pressure valve is closed and the high pressure valve is opened. As a result, high pressure fluid is pumped to the load for only the top half of the piston stroke. Any displacement between zero and full can be achieved by delaying the introduction of high pressure into the cylinder for an appropriate fraction of the power stroke.

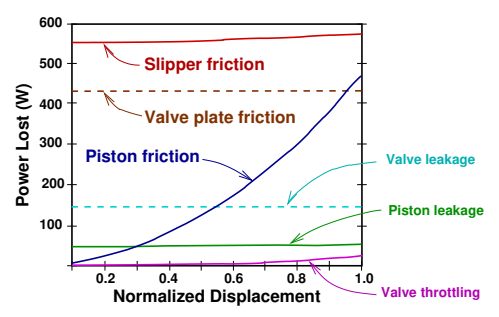
The operation of the PSPP motor is similar to that of the PSPP pump except that high pressure pressure is removed earlier during the motoring stroke to decrease displacement.

The reason that PSPP pump/motors operate more efficiently at low displacements than conventional pump/motors is explained in reference to Fig. 2. The figure compares the simulated losses in a conventional variable displacement swash plate pump/motor and a PSPP pump/motor with the same maximum displacements and operating at the same speed. The model used to perform the simulation is defined in Chapter 5 of [6].

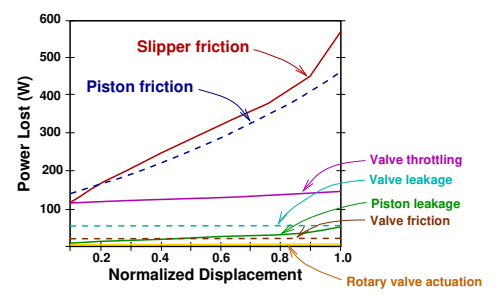
The losses in the swash plate pump/motor are illustrated in Fig. 2a. The two largest losses are attributable to slipper friction and valve plate friction. Since the force applied to the slipper remains high throughout the power stroke when the piston is pressurized, regardless of displacement, the power loss associated with slipper friction remains nearly constant. (The slipper friction power loss decreases slightly due to the change in swash plate angle.) Valve plate friction is also independent of displacement. As displacement is reduced, the power output of the pump decreases, but the two highest losses remain nominally constant. Therefore, efficiency declines as displacement is decreased.

The losses in the PSPP pump/motor are illustrated in Fig. 2b. Since a valve plate is not used, the Valve plate friction is eliminated. Furthermore, since the fraction of a cycle over which a piston is subject to high pressure is reduced when displacement is reduced, power lost to slipper friction also drops with displacement. The remaining losses are relatively low. Therefore, losses drop with displacement, and overall efficiency remains high over a wide range of displacement.

Note that valve throttling loss in a PSPP pump/motor is higher than in a swash plate pump/motor. The increased loss is attributable to shuttling low pressure fluid out of the piston cylin-



(a) Swash plate pump. "Slipper friction" represents friction between the slipper and swash plate. "Valve plate friction" represents friction between the valve plate and barrel. "Piston friction" represents friction between the outer diameter of the piston and the inner diameter of the cylinder.



(b) PSPP pump. "Slipper friction" represents friction between the slipper and wobble plate. "Piston friction" represents friction between the outer diameter of the piston and the inner diameter of the cylinder. "Valve friction" represents friction between the rotary valve and its sleeve.

FIGURE 2: Simulated losses in 48cc pumps operating at 20 MPa and 1800 RPM

der during a portion of the upstroke of the piston. However, the peak value of the valve throttling loss is a small fraction of the loss due to valve plate friction in a swash plate pump/motor.

Each cylinder of the PSPP pump/motor requires one or more valves to delay the introduction of high pressure into the piston cylinder for a prescribed fraction of the power stroke. The novel aspect of the pump described in this paper is the valve control mechanism. Previous embodiments of PSPP pumps have utilized either electrohydraulic valves [2] or cam-driven valves [8] as the control valve.

In contrast, the pump described here utilizes a rotary hydromechanically controlled valve. The overall architecture for one cylinder is illustrated in Fig. 3. Details of the valving concept are presented in [7].

Figure 4 illustrates actual pressure traces from one cylinder of the prototype PSPP pump/motor in the pumping mode. "Tank" represents pressure in the low pressure supply, "pilot" represents pilot pressure, and "high" represents the high pressure

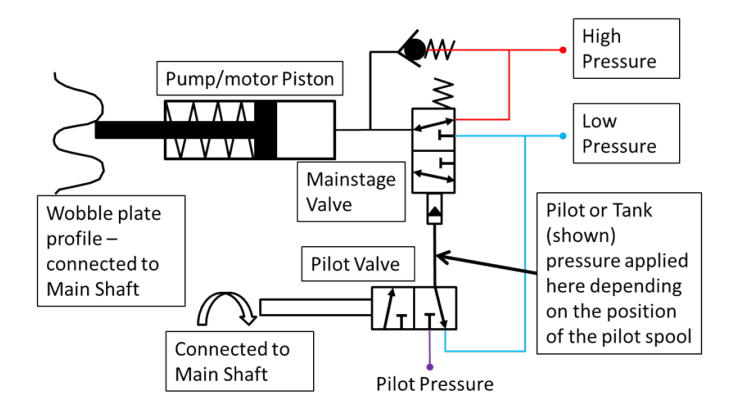


FIGURE 3: Hydraulic schematic of prototype

at the pump outlet. "Mainstage" represents the pressure at the outlet of the rotary valve and driving the main stage spool valve; it is nominally equal to either tank pressure or pilot pressure. "Chamber" represents the pressure in the piston cylinder.

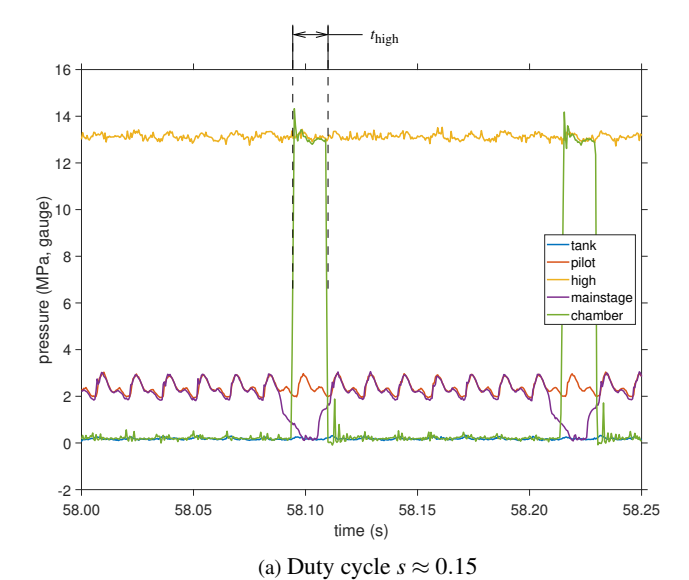
The prototype is designed so that the main stage valve connects the piston cylinder to tank pressure when the main stage pressure is high (e.g., pilot pressure). Conversely, the main stage valve connects the piston cylinder to high pressure when the main stage pressure is low (e.g., tank pressure). The pressure traces shown in Fig. 4 confirm this behavior.

"Duty cycle", s, is defined as the fraction of theoretical displacement delivered by the pump; e.g., if the pump is run at a duty cycle of s=0.5, it is delivering half of its theoretical displacement. Duty cycle is determined by the axial position of the rotary valve. Figure 4a corresponds to a duty cycle of approximately s=0.15. Figure 4b corresponds to a duty cycle of approximately s=0.86. Note that the period of the pulses between Fig. 4a and Fig. 4b is approximately the same, but the time that the spool valve connects the piston cylinder to high pressure during the power stroke increases for higher duty cycles.

DESIGN OF PROTOTYPE

Figure 5 shows a cutaway CAD model of the pump prototype. The overall architecture can be subdivided into two main functional sub-assemblies: the pump/motor and the controller. The design of the pump/motor subassembly is based on an existing conventional wobble plate pump. The pump/motor has eight pistons. Its theoretical displacement is $D_{th} = 47.5$ cc/rev and each piston has a diameter of 17.9 mm.

The controller subassembly is novel. The pump/motor requires only one rotary pilot valve to control all eight pistons. The rotary pilot valve is rotated by a tri-cornered shaft that is in turn rotated by the main shaft. The TDC position on the rotary pilot valve approximately aligns with the TDC of one of the pistons (see "Shaft Timing Angle and Pump Displacement" below). The



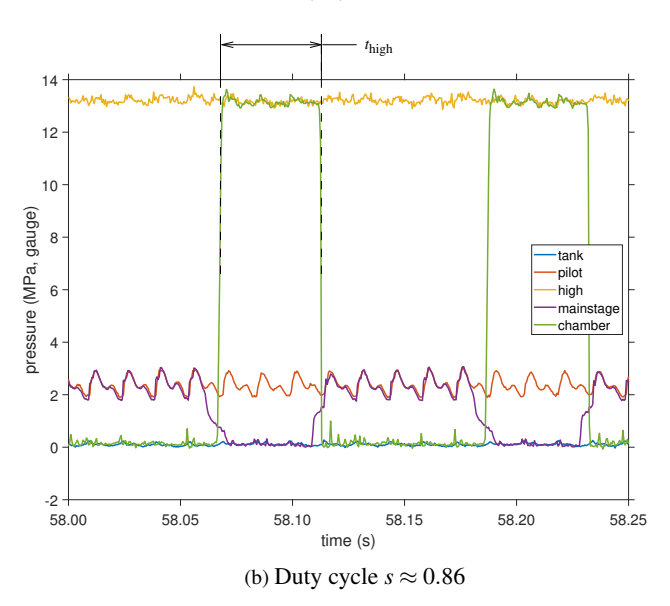


FIGURE 4: Pressure traces from the prototype pump operating at 13 MPa (2000 PSI) and 500 RPM

tri-cornered shaft has a sliding fit with a matching cavity in the interior of the rotary pilot valve, so the rotary valve can translate axially. The axial position of the rotary valve, which determines the duty cycle of the pump/motor, is set by a displacement adjustment mechanism.

Each piston is equipped with its own main stage valve. The sleeve of the rotary valve has eight output ports equally spaced about its periphery. Each outlet port supplies a small hydraulic piston that moves a main stage valve. When an actuator piston is supplied with pilot pressure, its main stage valve moves to a position where it connects a piston cylinder to low pressure. When

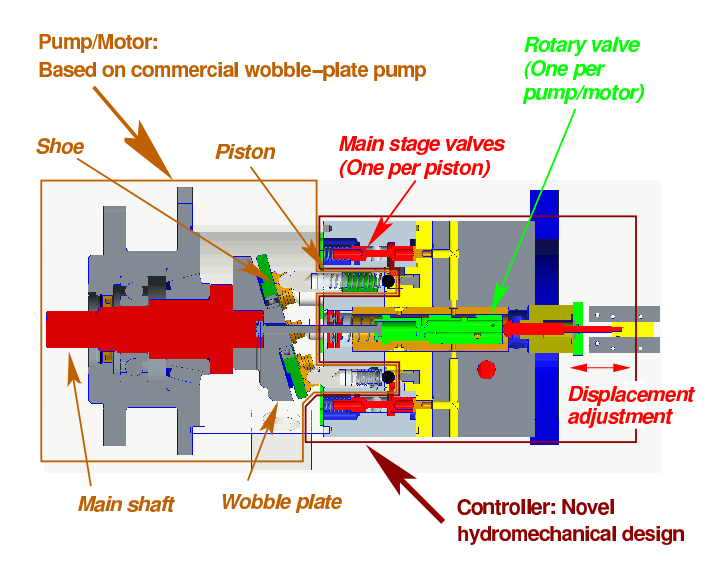


FIGURE 5: CUTAWAY CAD MODEL

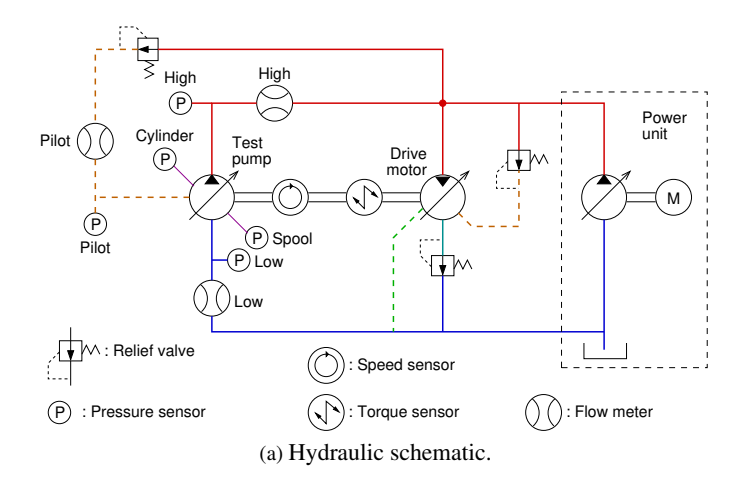
an actuator piston is supplied with low pressure, a return spring moves the main stage valve to a position where it connects a piston cylinder to high pressure. A small dead zone exists between the high and low pressure positions that can be used to achieve pre-compression and de-compression.

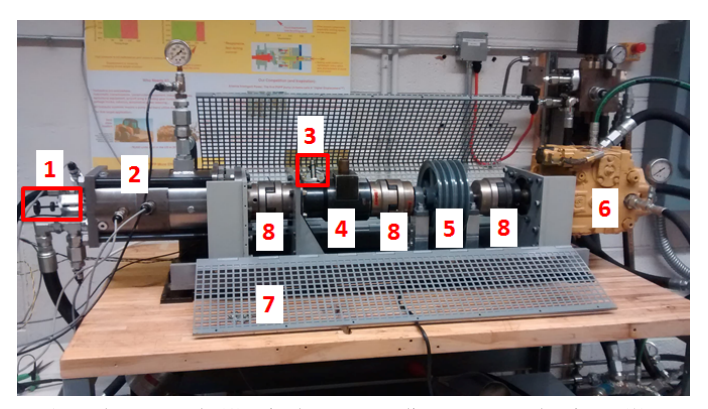
EXPERIMENTAL SETUP AND TESTING PROCEDURE Test Stand

The performance of the prototype pump was measured on the test stand illustrated in Fig. 6. The test stand employs a commercial closed circuit pump/motor (Sauer Danfoss Model 90R100, having a displacement of 100 cc/rev), used as a motor, to drive the prototype pump. The test stand is regenerative; e.g., high pressure fluid emanating from the prototype pump is channeled back to drive the motor. The prototype pump is augmented with a lab power unit (MTS Model 505.20, with flow rate 1300 cc/s) to make up for losses in the regenerative circuit. A hydraulic schematic of the test stand is shown in Fig. 6a.

Mechanical components employed in the test stand are labeled in Fig. 6b. The system speed is set by controlling the displacement of the motor. A shaft coupler connects the test pump to a torque sensor with an integrated speed sensor. A flywheel is included between the motor and the torque sensor to provides mechanical inertia; the flywheel stabilizes the system controller.

Pressure sensors are included on the high pressure rail, the low pressure rail, the pilot line of the pump, one of the piston cylinders, and an internal passage on the prototype pump which connects an orifice of the rotary valve to the main stage valve of the instrumented cylinder. Flow is measured at the low pressure port into the prototype pump, the high pressure port out of the prototype pump, and the pilot port into the prototype pump.





(b) Actual test stand. (1) Displacement adjustment mechanism. (2) Prototype pump/motor. (3) Speed sensor. (4) Torque sensor. (5) Flywheel. (6) Driving hydraulic motor. (7) Safety cage (closed while operating). (8) Shaft couplers.

FIGURE 6: Test stand architecture.

All electronic signals are sent to a DAQ that is driven by a Matlab/Simulink Real-time based controller. The controller is configured as a simple PI controller to control shaft speed.

Performance of the base pump/motor

The friction and leakage characteristics of the base pump/motor unit was first investigated to evaluate the potential performance of pump/motor at partial displacements using PSPP.

A friction test was conducted with the rotary valve's axial position corresponding to 0 displacement while the pump/motor is rotated at constant speed, and the friction torque is recorded with pilot pressure turned on or off. When the pilot pressure is turned on, the pump/motor operates normally at 0 displacement so that all the pistons are exposed to tank pressure. In contrast, when pilot pressure is removed, the main stage valves of all the pistons are exposed to high pressure. The torque recorded with pilot pressure on corresponds to the pressure independent friction

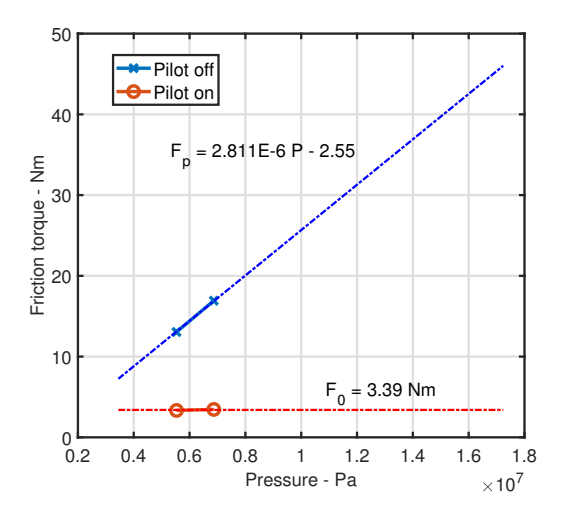


FIGURE 7: Friction torque at various system pressure with pilot pressure on (F_0) and off (F_p) and the unit is rotating at 500 RPM.

whereas the increase in torque when pilot pressure is removed corresponds to the additional friction when pressure is imposed all pistons. The results of these two torques at different system pressures are shown in Fig. 7.

If F_0 is the pressure independent friction and F_p is the friction when all pistons are pressured, then a rough estimate of the friction when the pistons are pressurized over a fraction of the stroke is:

$$F_{PSPP}(x) = F_0 + \frac{x}{2}(F_p - F_0)$$
 (1)

where the factor of 2 is due to the fact that only half of the pistons are under PSPP and the other half are not pressurized. Here x/2 is the fraction of the full *cycle period* that the pistons are exposed to high pressure. Because of the sinusoidal piston motion, x and the duty cycle s are related by:

$$s = \frac{1}{2}(1 - \cos(\pi x)) \tag{2}$$

The leakage of the base pump/motor unit is obtained by measuring the leakage at various system pressures when the pump/motor is not rotating (see Fig. 8). The leakage is modeled as:

$$Q_{leak} = k(P_{high} - P_0) \tag{3}$$

and k and P_0 are determined from the slope and y-intercept of the best-fit line shown in Fig. 8 ($k = 9.45 \times 10^{-7}$ cc/s/Pa and $P_0 = 1.29$ MPa). The leakage with pilot pressure on and off are very similar, indicating that predominant leakage is in the main stage valve, instead of from the piston chambers. Consequently, PSPP is not expected to reduce the leakage effect significantly.

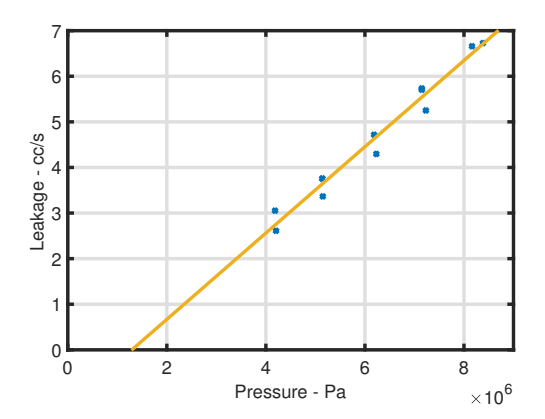


FIGURE 8: Leakage flow at various pressures at 0 displacements. The blue dots represent experimentally measured data points. The yellow line represents a linear fit.

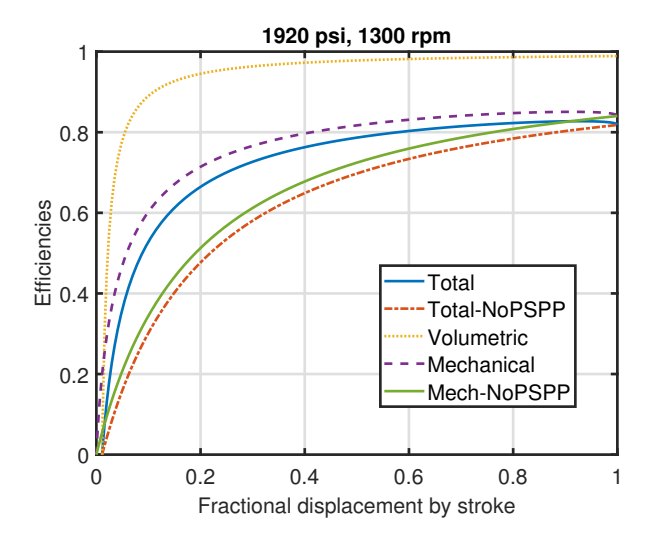


FIGURE 9: Efficiency versus displacement curves estimated from base unit friction and leakage with and without PSPP at 13.2 MPa (1920psi) and 1300 rpm.

The total, volumetric and mechanical efficiencies expected using the friction torque experimentally deduced from Fig. 7 and the leakage experimentally deduced from Fig. 8 is illustrated in Fig. 9. The "Total", "Volumetric" and "Mechanical" curves correspond to a PSPP pump. The "Total-NoPSPP" and "MechNoPSPP" curves correspond to a conventional variable displacement motor. The friction force is assumed to decrease with displacement according to Eqn. (1) for the PSPP pump, while it is assumed to remain constant in the conventional pump. In both cases, leakage is assumed to be constant.

The mechanical efficiency of the pump at full displacement is only 80%. The loss is attributed to friction at the wobble plate.

This loss was unexpected, as a set of bearings are intended to allow the wobble plate to rotate freely with respect to the shoe plate, which in turn contacts the piston shoes. The high loss indicates that the bearings may not be functioning as intended.

Nevertheless, with PSPP, the efficiency at full displacement is expected to be substantially maintained over a broad range of displacements. PSPP is expected to raise the total efficiency by 20% relative to a conventional pump having the friction torque properties shown in Fig. 7 at the displacement ratio of 0.2. It is interesting to note that the model predicts that the peak efficiency occurs at slightly below full displacement. The reason is that the pressure dependent friction varies with the fraction of the cycle period that the piston is pressurized, x/2, whereas the output power varies with the duty cycle, s.

Testing Procedure

Each time a data-collection test is run, the displacement of the prototype pump is set, and then the motor is taken through a range of speeds and held at each speed for several seconds. The displacement of the prototype pump is set by manually changing the axial position of the rotary pilot valve.

The efficiency is determined from the actual torque required to drive the pump and the actual pressure and flow developed by the pump:

$$eff = \frac{PQ_{act}}{T\omega} \tag{4}$$

where P is the output pressure, Q_{act} is the output flow in cubic meters per second, T is the input torque in Newton meters, and ω is the shaft speed in radians per second. The normalized displacement, $S_{norm} \in [0,1]$ which corresponds to the fraction of full theoretical output flow is given by:

$$S_{norm} = \frac{2\pi Q_{act}}{\omega D_{th}} \tag{5}$$

where D_{th} is the theoretical displacement per revolution.

Shaft Timing Angle and Pump Displacement

The prototype pump-motor is equipped with a set screw adjustment that enables changing the relative angle between the rotary pilot valve and the wobble plate between test runs. It can be used to adjust valve timing due to delay between pilot stage valve events and the main-stage valve events.

The delay time of the spool valve pilot system, $t_{\rm delay}$, is formally defined to be the time interval between when the pilot valve pressure crosses the midway point between tank and pilot pressure, and when the piston chamber pressure drops to midway between high and tank pressure. (Recall that the cylinder

pressure is nominally high when pilot pressure is low and vice versa.) Note that the amount that the shaft rotates during this delay, $\Delta\theta_{\rm delay}$, is a function of shaft speed:

$$\Delta \theta_{\rm delay} = t_{\rm delay} \omega \tag{6}$$

The main stage valve delay time of the prototype pump has been estimated to be 3 ms [6]. At 1000 RPM, this delay results in the pressure in the piston chambers switching from high to low 18° after TDC. Changing the set screw adjustment varies the offset angle, α , between the TDC positions on the wobble plate and on the rotary valve spool. If the offset angle were set to -18° , the pump chamber would open to low pressure exactly at TDC at 1000 RPM.

The valve delay and the offset angle affect the effective displacement from the pump, as illustrated in Fig. 10. The cylinder pressure is assumed to drop from high to low pressure at a shaft angle of:

$$\theta_2 = 2\pi + t_{\text{delay}}\omega + \alpha \tag{7}$$

The pumping stroke is assumed to end at angle θ_2 . Note, however, that if θ_2 falls after 2π , as shown in the figure, a short interval of motoring may actually occur between 2π and θ_2 . Therefore, the shaft angle where pumping begins is assumed to be:

$$\theta_1 = 2\pi + t_{\text{delay}}\omega + \alpha - t_{\text{high}}\omega$$
 (8)

where t_{high} represents the time that the cylinder remains at high pressure (see Fig. 4). The estimated fractional displacement, S_{est} , accounting for the valve delay time and offset angle, is therefore:

$$S_{est} = \frac{1}{2} (cos(t_{\text{delay}}\omega + \alpha) - cos((t_{\text{delay}} - t_{\text{high}})\omega + \alpha))$$
 (9)

whereas x, the fraction of the pumping stroke in time when the pistons are exposed to high pressure, in (1) is $x = \omega t_{\text{high}}/\pi$.

Note that (9) typically gives a slightly different fractional displacement than that given by (5) due to timing offset, leakage and compressibility. Since (5)) is more comprehensive, the normalized displacement is used as the abscissa for the efficiency and power loss graphs provided in the following sections. Note, however, that no real pump will be able to achieve a normalized displacement of 1.0.

RESULTS

Effect of offset angle

Setting the offset angle of the prototype pump/motor is quite laborious. System efficiencies at a few offset angles are shown in is shown in Fig. 11.

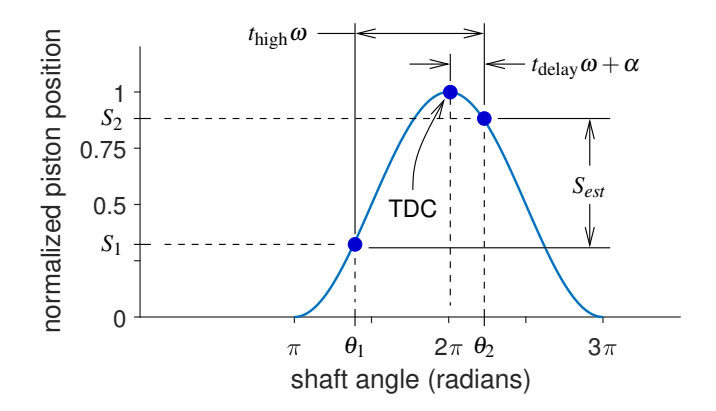


FIGURE 10: Estimation of pump displacement while accounting for main stage valve actuation delay and offset angle.

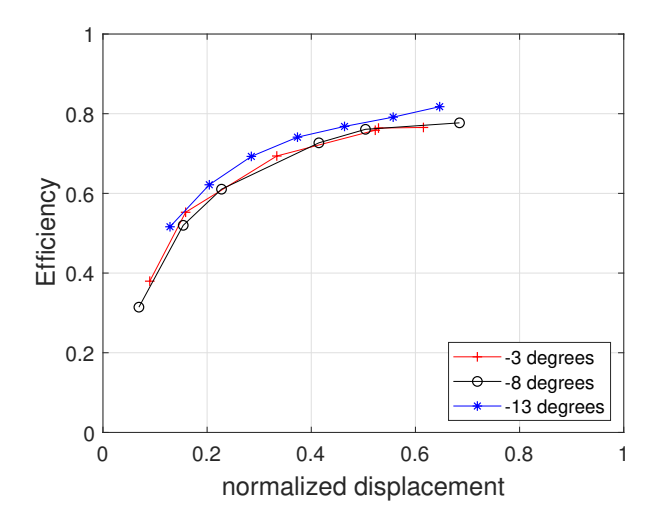


FIGURE 11: Efficiency vs. displacement for three offset angles at 900 RPM and 10 MPa (1500 PSI)

The efficiency typically varied only slightly between offset angles of -13° , -8° and -3° . Nevertheless, an offset angle of -13° consistently produced the highest efficiencies. Therefore, an offset angle of -13° was used for the remainder of testing. If a valve delay of 3 ms is assumed, the -13° offset angle corresponds to opening the piston cylinder to low pressure 5° past TDC at a shaft speed of 1000 RPM.

The relative insensitivity of efficiency to offset angle is likely attributable to the fact that the compressible volume of fluid in the piston cylinder is minimized at TDC. Therefore, little fluid flows through the spool valve at the end of the pumping stroke regardless of mismatches between the cylinder and tank pressures.

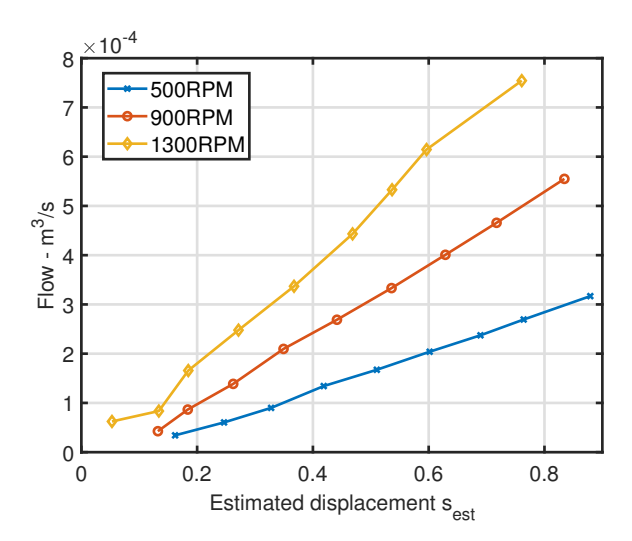


FIGURE 12: Output flow versus fractional displacement at 14 MPa (2000Psi)

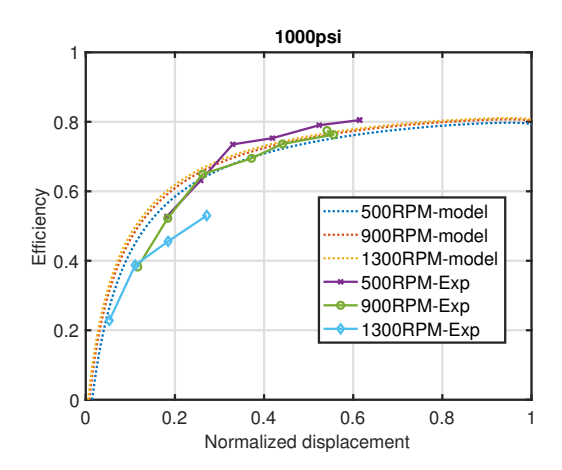


FIGURE 13: Predicted and measured efficiency vs. normalized displacement for three speeds at 7 MPa (1000 Psi)

Output Flow versus displacement

Figure 12 presents the relationship between output flow and fractional displacement at 1200 RPM. It shows that indeed increasing fractional displacement by increasing the fraction of stroke that the pistons are exposed to high pressure increases the output flow nearly proportionally.

Efficiency versus displacement

The overall efficiency of the pump for a series of increasing operating pressures is illustrated in Figs. 13-16. Experimentally measured efficiency data is compared with results from a model using the estimated pump properties utilized to generate Fig. 9. The model is developed in Chapter 5 of [6].

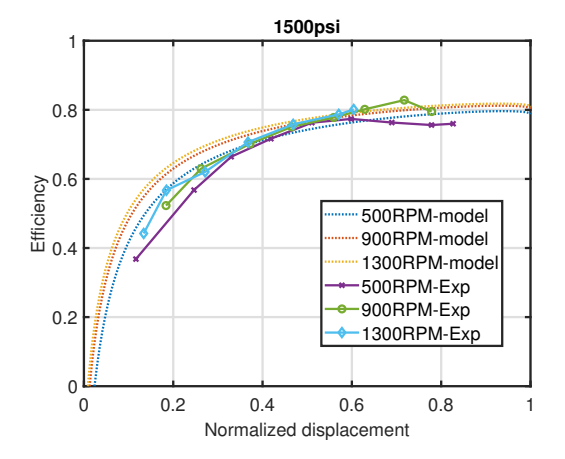


FIGURE 14: Predicted and measured efficiency vs. normalized displacement for three speeds at 10 MPa (1500 Psi)

Figure 13 reveals that a limited range of displacements were achieved for a high pressure of 7 MPa. The cause was the usage of a closed circuit hydraulic motor to power the pump (see Fig. 6). Raising the low pressure side of the motor to charge pressure caused the pressure differential across the motor to be insufficient to turn the pump at normalized displacements over about 0.5. Nevertheless, the data points that were obtained were consistent with the model predictions.

The total efficiency versus displacement is largely consistent for high pressures of 10 MPa (Fig. 14), 13 MPa (Fig. 15), and 17 MPa (Fig. 16). The efficiency curves remain quite flat from normalized displacements of about 50% to the maximum achievable. It is noted that the highest displacements achievable for each pressure were limited by ultimate stalling of the driving motor. (Increasing the power of the driving motor would enable taking the pump to slightly higher displacements.)

Even with the high mechanical losses evident in the prototype, the experimentally measured efficiency at 20% displacement is still around 50%. All experimentally measured efficiencies are largely consistent with predictions of the model.

Figure 17 shows experimentally measured total efficiency at three different operating pressures for a pump speed of 1000 RPM. The offset angle was nominally optimized for this speed. The total efficiency remains largely flat, at about 80%, for displacements of 40% to the maximum achievable. Even with the poor mechanical efficiency of the prototype, the efficiency hovers at around 50% at a displacement of only 10%. The efficiencies appear to have the general trend of increasing with pressure, with a more noticeable drop-off at the lowest pressure of 7 MPa.

Power loss versus displacement

Power loss as a function of normalized displacement is investigated for various operating pressures in Fig. 18-Fig. 21.

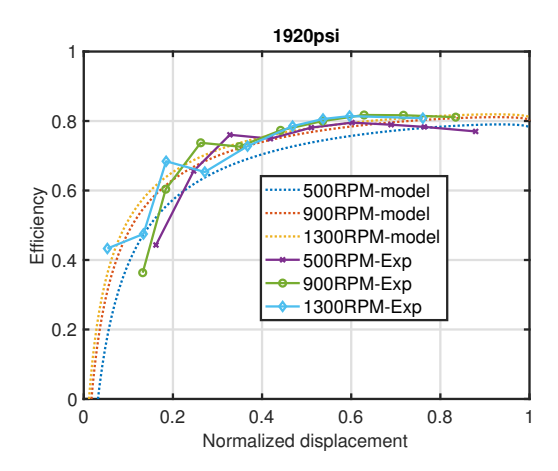


FIGURE 15: Predicted and measured efficiency vs. normalized displacement for three speeds at 13 MPa (1920 Psi)

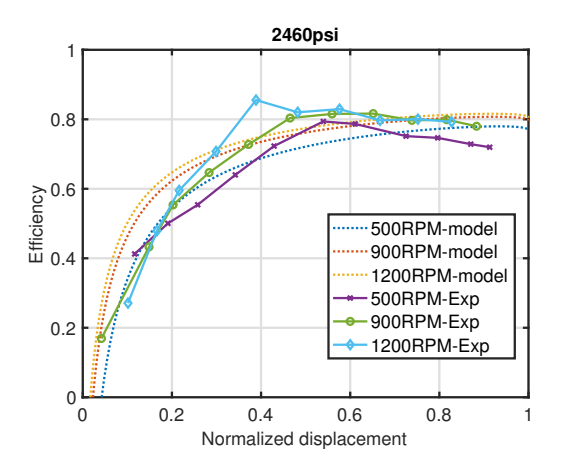


FIGURE 16: Predicted and measured efficiency vs. normalized displacement for three speeds at 17 MPa (2460 Psi)

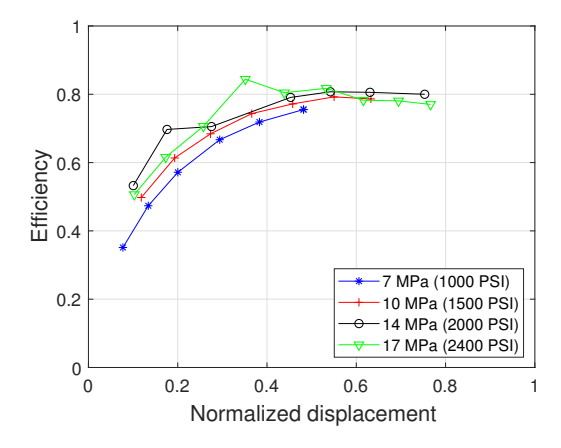


FIGURE 17: Efficiency vs. normalized displacement for three pressures at 1000 RPM

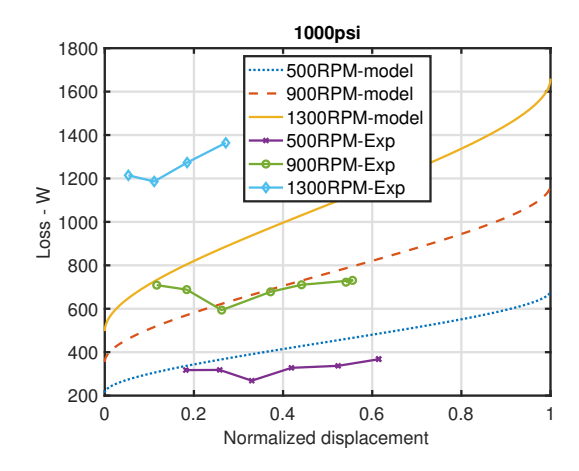


FIGURE 18: Predicted and measured power loss vs. displacement for three speeds at 7 MPa (1000 PSI)

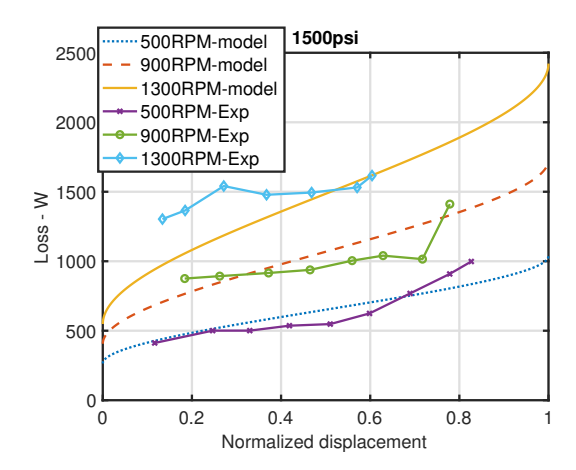


FIGURE 19: Predicted and measured power loss vs. displacement for three speeds at 10 MPa (1500 PSI)

Each Figure shows the results for a range of operating speeds. These figures show that power losses do indeed decrease as displacements decrease, as predicted from the friction/leakage models. The power loss predictions tend to be somewhat more accurate at lower speeds.

DISCUSSION

The experiments reviewed here validate the concept of a hydromechanically driven partial stroke piston pressurization pump. Unfortunately, mechanical losses associated with the wobble plate pump subsystem of the first prototype (see Fig. 7) limited the overall pump efficiency to about 80%. However, those losses are in no way attributable to the novel PSPP control subsystem. Indeed, the first prototype demonstrated that nearly constant efficiency was maintained from displacements

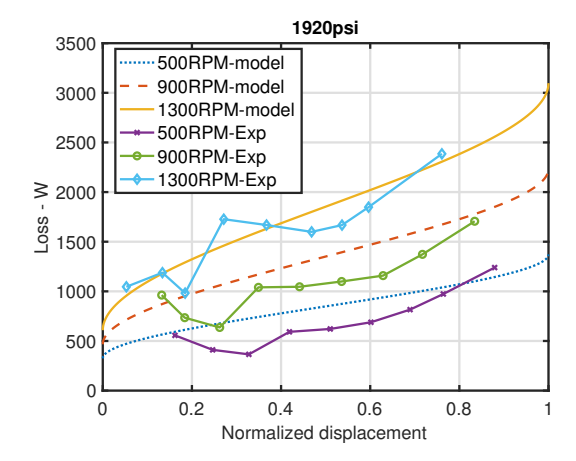


FIGURE 20: Predicted and measured power loss vs. displacement for three speeds at 13.2 MPa (1920 PSI)

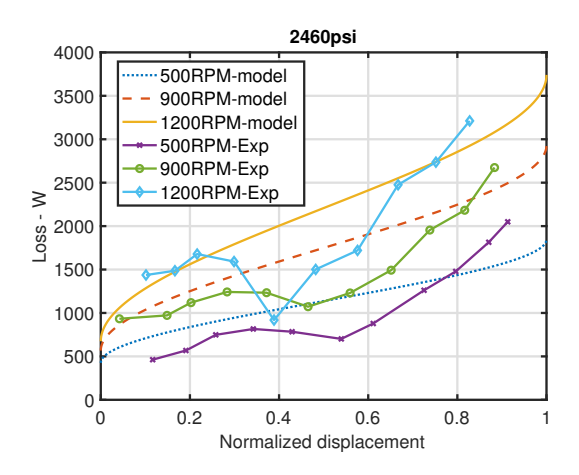


FIGURE 21: Predicted and measured power loss vs. displacement for three speeds at 17 MPa (2460 PSI)

of around 50% to full, and good efficiency was maintained to displacements as low as about 10%.

The power consumed by the pilot system is not included in the efficiencies stated in this paper. The pilot system power was not calculated because excessive leakage was observed in the pilot system, likely due to excessive clearances between the spool valve actuator pistons and their sleeves. The power consumption of the pilot system is expected to be very low in a properly manufactured pump (see Fig. 2).

The hydromechanical valving system demonstrated in the scope of this paper can easily be implemented on improved base pump architectures. Therefore, hydromechanical PSPP appears to offer a promising means for achieving high efficiency cost effectively in variable displacement pumps.

CONCLUSION

Experimental testing results for a novel variable displacement pump/motor run in pumping mode have been presented. The prototype pump/motor uses a 2D rotary valve to hydromechanically adjust the on/off valve timing to connect and remove pressure to the pistons according to desired displacement. It is shown that despite the base unit having a substantial friction, high efficiency can be maintained even at low displacements of 10-20% using the partial stroke pressure pressurization concept. Comparison of the efficiencies and power losses with predictions based on the friction and leakage characteristics of the base unit indicate that the PSPP concept is working as expected.

Future work will include testing of the pump/motor in motoring mode and investigating the source of high friction in the wobble plate subsystem of the base unit.

ACKNOWLEDGMENT

This material is based upon work supported by the National Science Foundation under Grant #PFI-1700747 and through the Center for Compact and Efficient and Fluid Power (CCEFP) under Grant #EEC-0540834.

REFERENCES

- [1] Rampen, W., and Salter, S. "The Digital Displacement Hydraulic Piston Pump," Proc. of the 9th International Symposium on Fluid Power, Cambridge, England, 1990.
- [2] M. Ehsan, W. Rampen and S. Salter, "Modeling of Digital-Displacement Pump-Motors and Their Application as Hydraulic Drives for Nonuniform Loads", ASME J. of Dynamic Systems and Control, Vol. 122, pp. 210-215, 2000.
- [3] Merrill, K. "Modeling and Analysis of Active Valve Control of a Digital Pump/Motor," Ph.D. Thesis, Purdue University, West Lafavette, IN, 2012.
- [4] Holland, M., "Design of Digital Pump/Motors and Experimental Validation of Operating Strategies," Ph.D. Thesis, Purdue University, West Lafayette, IN., 2012.
- [5] Tammisto, J., Huova, M., Heikkila, M., Linjama, M., and Huhtala, K. "Measured Characteristics of an In-line Pump with Independently Controlled Pistons," 7th International Fluid Power Conference, Aachen, Germany, 2010.
- [6] M. B. Rannow. Achieving Efficient Control of Hydraulic Systems Using On/Off Valves. Ph.D. Thesis, University of Minnesota, 2016.
- [7] M. B. Rannow, P. Y. Li and T. R. Chase, "Discrete Piston Pump/Motor Using a Mechanical Rotary Valve Control Mechanism", Proc. of the 8th Workshop on Digital Fluid Power (DFP16), Tampere, Finland, May 24-25, 2016.
- [8] T. Helmus, F. Breidi, and J. Lumkes, "Simulation of a Variable Displacement Mechanically Actuated Digital Pump Unit", Proc. of the 8th Workshop on Digital Fluid Power (DFP16), Tampere, Finland, May 24-25, pp. 95-105, 2016.